J. Fluid Mech. (1997), *vol.* 340, *pp.* 61–82. Printed in the United Kingdom

© 1997 Cambridge University Press

Mass transport in viscous flow under a progressive water wave

By ALLAN W. GWINN AND S. J. JACOBS

Department of Atmospheric, Oceanic and Space Sciences, The University of Michigan, Ann Arbor, MI 48109-2143, USA

(Received 19 June 1996 and in revised form 10 December 1996)

We consider two-dimensional free surface flow caused by a pressure wavemaker in a viscous incompressible fluid of finite depth and infinite horizontal extent. The governing equations are expressed in dimensionless form, and attention is restricted to the case $\delta \ll \epsilon \ll 1$, where δ is the characteristic dimensionless thickness of a Stokes boundary layer and ϵ is the Strouhal number. Our aim is to provide a global picture of the flow, with emphasis on the steady streaming velocity.

The asymptotic flow structure near the wavenumber is found to consist of five distinct vertical regions: bottom and surface Stokes layers of dimensionless thickness $O(\delta)$, bottom and surface Stuart layers of dimensionless thickness $O(\delta/\epsilon)$ lying outside the Stokes layers, and an irrotational outer region of dimensionless thickness $O(1)$. Equations describing the flow in all regions are derived, and the lowest-order steady streaming velocity in the near-field outer region is computed analytically.

It is shown that the flow far from the wavemaker is affected by thickening of the Stuart layers on the horizontal length scale $O[(\epsilon/\delta)^2]$, by viscous wave decay on the scale $O(1/\delta)$, and by nonlinear interactions on the scale $O(1/\epsilon^2)$. The analysis of the flow in this region is simplified by imposing the restriction $\delta = O(\epsilon^2)$, so that all three processes take place on the same scale. The far-field flow structure is found to consist of a viscous outer core bounded by Stokes layers at the bottom boundary and water surface. An evolution equation governing the wave amplitude is derived and solved analytically. This solution and near-field matching conditions are employed to calculate the steady flow in the core numerically, and the results are compared with other theories and with observations.

1. Introduction

Steady streaming motions in predominantly oscillatory flows are generated by Reynolds stress forces acting in boundary layers and other regions of the fluid where viscous effects are significant (Lighthill 1978). Although this phenomenon has been understood in general terms since Lord Rayleigh's work in nonlinear acoustics (Rayleigh 1945, pp. 333–342), the role played by streaming motions in the theory of water waves and in other wave propagation problems is sufficiently important to justify further study of the subject.

In the present paper we consider viscous free surface flow caused by an oscillating surface pressure in an incompressible fluid of finite depth and infinite horizontal extent. We define this oscillating surface pressure as a pressure wavemaker. The studies on which we base our work are the computation by Longuet-Higgins (1953) of the matching conditions at the outer edges of the Stokes boundary layers at the bottom boundary and the water surface, Stuart's (1966) analysis of the mean flow transition

https://doi.org/10.1017/S002211209700520X Published online by Cambridge University Press

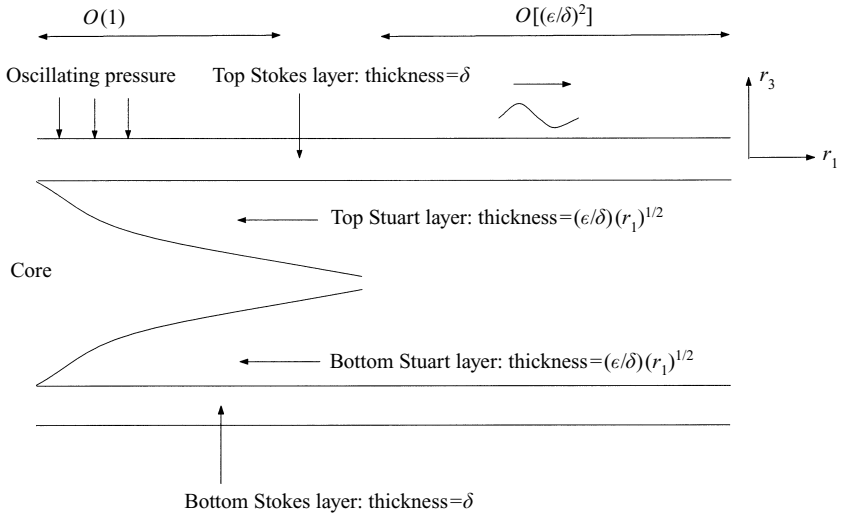


FIGURE 1. Schematic diagram of the asymptotic structure.

layers adjacent to the Stokes layers, Davey & Stewartson's (1974) derivation of the nonlinear Schrödinger equation governing the amplitude of a monochromatic water wave, Van Dyke's (1970) treatment of viscous entry flow in a channel, and the derivations by Dore (1976) and Leibovich (1980) of the equations governing steady streaming outside the Stokes layers. Our aim is to fit these results together to provide a global picture of the flow, with emphasis on the steady streaming velocity. In particular, we will show that the inviscid solution of Stokes (1847) provides a fair approximation to the mean horizontal velocity profile close to the wavemaker, while the flow far from the wavemaker is described with good accuracy by the viscous theory of Longuet-Higgins, as amended by Craik (1982).

Our work differs from recent numerical computations of streaming motions associated with water waves (Iskandarani & Liu 1991*a*, *b*, 1993; Wen & Liu 1994), since the waves treated in these studies are periodic in the propagation direction, and decay temporally but not spatially. In more closely related papers, Dore (1977) obtains an *ad hoc* similarity solution for the mean flow valid only for fluids of infinite depth, and Liu & Davis (1977), Grimshaw (1981), and Craik (1982) treat flows for which a typical wave amplitude is small compared to the thickness of a Stokes layer. In the present study we extend these theories by obtaining a solution for finite-depth fluids and for wave amplitudes significantly larger than those considered by Liu & Davis, Grimshaw, and Craik.

In figure 1 we show the experimental set-up and the asymptotic flow structure. To explain our reasons for proposing this structure, we define the reciprocals of a characteristic wavenumber and frequency as length and time scales, r_1 and r_3 as dimensionless coordinates measuring distance along and perpendicular to the mean surface level, δ as the dimensionless thickness of the Stokes layers, and ϵ as the Strouhal number, the ratio of the advective terms in the momentum equations to the time-derivative terms. We consider flows driven by an imposed normal stress at the water surface, where the imposed stress is sinusoidal in time and vanishes as $|r_1| \to \infty$, and we neglect transients by taking the dependent variables to be temporally periodic. In addition, we restrict our attention to the case $d = O(1)$ and $\delta \ll \epsilon \ll 1$, where d is the dimensionless ambient fluid depth. When expressed in this notation, the solutions given

https://doi.org/10.1017/S002211209700520X Published online by Cambridge University Press

by Liu & Davis, Grimshaw, and Craik hold only for $\epsilon \ll \delta$. In terminology employed by Longuet-Higgins, their analysis applies only to the conduction case while ours applies more generally and contains both the conduction and convection solutions as special cases.

In essence, Rayleigh's method of solution consists of expanding the dependent variables in powers of ϵ to obtain a sequence of linear problems. If the present flow is treated in this way, we find that the $O(1)$ solution is sinusoidal in time and that the $O(\epsilon)$ solution is the sum of a steady flow and a double harmonic. Up to and including $O(\epsilon)$ terms, the transient part of the solution consists of an inviscid irrotational core flow bounded by Stokes layers at the boundaries.

The $O(\epsilon)$ mean flow is inviscid and presumably irrotational because of the nature of the forcing, but must satisfy viscous boundary conditions if required to match the $O(\epsilon)$ Stokes layer solutions derived by Longuet-Higgins. This implies that the mean vorticity decays to zero with distance from the boundaries in Stuart layers lying outside the Stokes layers, which in turn implies that the outer flow cannot be irrotational everywhere because the Stuart layers thicken with distance from the wavemaker, and ultimately include the entire water column. Hence, in our view the horizontal asymptotic structure consists of two distinct regions: a near field close to the wavemaker in which the outer flow is inviscid and irrotational, and a far field in which viscous effects play a major role throughout the fluid. In addition, each of the horizontal regions divides into a bottom boundary layer, an outer core flow, and a surface boundary layer.

The flow structure can be described quantitatively by defining L_H and L_V as horizontal and vertical Stuart layer length scales, and by noting that solution of the linear inviscid wavemaker problem shows that the $O(\epsilon)$ mean flow is the sum of a term independent of r_1 and of an infinite series S of terms that decay exponentially in $|r_1|$ with $O(1)$ decay constants. The presence of the series S imposes the length scale $L_H = 1$, and balancing advective and viscous terms in the temporally averaged equations yields $L_V = \delta/\epsilon$, where, to repeat, δ is the Stokes layer thickness and ϵ is the Strouhal number. Consequently, we find that the near-field flow structure consists of Stokes layers at the bottom boundary and water surface of characteristic length scale δ, adjacent Stuart layers, which apply only to the mean flow field and have dimensionless thickness δ/ϵ, and an inviscid and irrotational core. Here the near field is defined as the region $|r_1| = O(1)$ in which the series S is $O(1)$ in magnitude.

Because this series decays with distance from the wavemaker, the near-field mean velocity just outside the Stokes layers becomes independent of r_1 as $|r_1| \to \infty$, and provides no information about the scale L_H. This comes instead from the Stuart layer equations, derived here in Appendix A, which suggest that the Stuart layers thicken with distance from the wavemaker in the same way as a Blasius boundary layer, and thus have a local scale $L_V = (\delta/\epsilon)\,|r_1|^{1/2}$. Therefore, since the Stuart layers fill the fluid when $L_V = 1$, the far field is the region $|r_1| = (\epsilon/\delta)^2$, and the far-field flow structure consists of Stokes layers at the boundaries and a viscous mean flow in the core. Figure 1 is based on the above reasoning, and closely resembles figure 1 in Van Dyke's study of channel entry flow.

In addition to the scale $(\epsilon/\delta)^2$, two other large horizontal length scales are significant. There are $1/\epsilon^2$, the wave interaction length scale implied by Davey & Stewartson's (1974) derivation of the nonlinear Schrödinger equation for monochromatic water waves, and $1/\delta$, the horizontal scale on which temporally sinusoidal water waves decay in a viscous fluid of finite depth. We find, then, that three large length scales play a role in the analysis, namely $(\epsilon/\delta)^2$, the length required for the Stuart layers to fill the fluid,

https://doi.org/10.1017/S002211209700520X Published online by Cambridge University Press

and the lengths $1/\epsilon^2$ and $1/\delta$, which govern the variation of the wave field with distance from the wavemaker.

To simplify our analysis of the far-field flow, we consider a parameter setting such that wave decay, nonlinear interactions, and thickening of the Stuart layers all take place on the same scale. This occurs if

$$\delta = \lambda\epsilon^2, \tag{1.1}$$

where λ is an $O(1)$ constant. For this case the near and far fields are the regions $|r_1| = O(1)$ and $|r_1| = O(1/\epsilon^2)$, respectively, and wave decay and nonlinear interactions both take place on the scale $1/\epsilon^2$.

In addition to its mathematical convenience, the parameter setting $\lambda = O(1)$ holds in many experimental situations. For example, typical values of the constants in a laboratory study of progressive waves are a kinematic viscosity of 0.01 $\mathrm{cm}^2\,\mathrm{s}^{-1}$, a wave period of 1 s, a depth of 50 cm, and a wave amplitude of 1.5 cm. Using (2.1) below, this gives $d \sim 2$, $\delta \sim 0.002$, $\epsilon \sim 0.06$, and so $\lambda \sim 0.6$, an $O(1)$ constant.

In the remainder of the paper we derive and solve the equations governing the lowest-order transient and mean flows in the near-field outer region for the case $d = O(1)$ and $\delta \ll \epsilon \ll 1$. To treat the far-field outer region we impose the additional restriction (1.1), with $\lambda = O(1)$. We then derive evolution equations for the temporally averaged velocity and the complex amplitude of the wave field, solve the latter equation analytically to determine the wave amplitude as a functional of the mean horizontal velocity, and use this result and near-field matching conditions to compute the lowest-order approximation for the mean flow numerically. The results are summarized and discussed in our concluding section.

2. Dimensionless equations of motion

Let $\boldsymbol{r} = (r_1, r_2, r_3)$ denote the position vector in Cartesian coordinates, with r_3 pointing in the vertical direction, and let t denote time. We consider two-dimensional flow in the (r_1, r_3)-plane between the water surface $r_3 = \zeta(r_1, t)$ and the solid bottom $r_3 = -D^*$ in a channel of infinite horizontal extent, with viscous effects included and surface tension omitted. Characteristic values of the wavenumber, the wave frequency, and the particle velocity are denoted here by κ^*, σ^* and V^*, respectively, where κ^* and σ^* are related through the deep-water dispersion relation. We scale lengths by $1/\kappa^*$, time by $1/\sigma^*$, the velocity $\boldsymbol{u}$ by V^*, the surface elevation ζ by V^*/σ^*, and the kinematic surface traction $\boldsymbol{f}$ and excess pressure p by $(V^*\sigma^*)/\kappa^*$. Three parameters arise after scaling: δ, a measure of viscous effects, the Strouhal number ϵ, a measure of nonlinearity, and the dimensionless depth d. Their definitions are

$$\delta = (2\nu\kappa^{*2}/\sigma^*)^{1/2}, \quad \epsilon = V^*\kappa^*/\sigma^*, \quad d = \kappa^* D^*, \tag{2.1}$$

respectively, where ν is the kinematic viscosity. We restrict our attention to the case $d = O(1)$ and $\delta \ll \epsilon \ll 1$.

When expressed in dimensionless form, the Navier–Stokes equations become

$$\frac{\partial u_k}{\partial r_k} = 0, \tag{2.2}$$

$$\frac{\mathrm{D}u_i}{\mathrm{D}t} + \frac{\partial p}{\partial r_i} = \frac{1}{2}\delta^2 \frac{\partial E_{ki}}{\partial r_k}, \tag{2.3}$$

https://doi.org/10.1017/S002211209700520X Published online by Cambridge University Press

where u_i are the Cartesian velocity components and

$$\frac{\mathrm{D}}{\mathrm{D}t} = \frac{\partial}{\partial t} + \epsilon u_k \frac{\partial}{\partial r_k}, \quad E_{ik} = E_{ki} = \frac{\partial u_i}{\partial r_k} + \frac{\partial u_k}{\partial r_i}. \tag{2.4}$$

The dimensionless boundary conditions are

$$u_i = 0 \quad \text{at} \quad r_3 = -d, \tag{2.5a}$$

$$(-p+\zeta)\, n_i + \tfrac{1}{2}\delta^2 n_k E_{ki} = f_i, \quad \frac{\mathrm{D}}{\mathrm{D}t}(r_3 - \epsilon\zeta) = 0 \quad \text{at} \quad r_3 = \epsilon\zeta, \tag{2.5b}$$

in which n_i and f_i are the unit outward-pointing normal to the water surface and the surface traction, respectively.

Our aim is to compute the flow forced by a pressure wavemaker, which we model by letting

$$f_i = n_i F = n_i\{a(r_1)\exp(-\mathrm{i}\sigma t) + \text{c.c.}\}, \tag{2.6}$$

where c.c. is the complex conjugate, a is an even function of r_1 satisfying $a(\pm\infty) = 0$, and σ is the dimensionless frequency of the wavemaker. In the calculation we omit treatment of transients by taking the dependent variables to be periodic functions of σt. Also, since the r_1-component of the horizontal velocity is odd in r_1 and the other dependent variables are even, we consider only the region $r_1 \geqslant 0$ in the analysis presented below.

Equations (2.2)–(2.5*a*) will be used to treat the bottom boundary layer, and the coordinates (x, z) and velocity components (u, w) defined by

$$r_1 = x, \quad r_3 = z + \epsilon\frac{z+d}{d}\zeta, \quad u = u_1, \quad w = u_3, \tag{2.7}$$

to treat the flow in the outer region. This flow will be analysed using Joseph's method of domain perturbations, and therefore, as explained by Joseph (1973) and Leibovitz (1982), it is unnecessary to express the governing equations in terms of the (x, z)-coordinates.

To treat the surface layer, we employ a moving orthogonal curvilinear coordinate system (s, n), where s and n are parallel and perpendicular to the water surface, respectively. The components of the particle velocity and the surface traction are denoted in this system by (u_s, u_n) and $(f_s, f_n) = (0, F)$, and the equation of the surface is $n = 0$.

With the exception of the fluid acceleration, all terms in the Navier–Stokes equations can be expressed in the (s, n)-coordinates through use of standard formulae. To determine the acceleration, we define $T = t$ and we let $\partial/\partial t$ denote the partial derivative with respect to time with (r_1, r_3) held fixed and $\partial/\partial T$ the derivative with (s, n) held fixed. Defining the (s, n)-coordinates by $\boldsymbol{r} = \boldsymbol{R}(s, n, T)$, with $\boldsymbol{R}$ a prescribed function of its arguments, and letting $\boldsymbol{c} = \partial\boldsymbol{R}/\partial T$, these derivatives are related by

$$\frac{\partial}{\partial t} = \frac{\partial}{\partial T} - \boldsymbol{c}\cdot\boldsymbol{\nabla}. \tag{2.8}$$

From (2.8) it follows that the material derivative operator takes the form

$$\frac{\mathrm{D}}{\mathrm{D}t} = \frac{\partial}{\partial T} + (\boldsymbol{u} - \boldsymbol{c})\cdot\boldsymbol{\nabla}. \tag{2.9}$$

https://doi.org/10.1017/S002211209700520X Published online by Cambridge University Press

Therefore, since $\partial\hat{\boldsymbol{s}}/\partial T = -\Gamma\hat{\boldsymbol{n}}$ and $\partial\hat{\boldsymbol{n}}/\partial T = \Gamma\hat{\boldsymbol{s}}$, where Γ is the angular speed of the (s,n)-coordinate axes, the acceleration takes the form

$$\frac{\mathrm{D}\boldsymbol{u}}{\mathrm{D}t} = \hat{\boldsymbol{s}}\left(\frac{\partial u_s}{\partial T} + \Gamma u_n\right) + \hat{\boldsymbol{n}}\left(\frac{\partial u_n}{\partial T} - \Gamma u_s\right) + (\boldsymbol{u}-\boldsymbol{c})\cdot\boldsymbol{\nabla}\boldsymbol{u}. \tag{2.10}$$

In the present problem we define s and n by

$$r_1 = s\frac{\epsilon n}{M}\frac{\partial\zeta}{\partial s}, \quad r_3 = \epsilon\zeta + \frac{n}{M}, \tag{2.11}$$

where ζ is expressed as a function of s and T, and where

$$M = [1+\epsilon^2(\partial\zeta/\partial s)^2]^{1/2}. \tag{2.12}$$

In this system the scaled equations of motion take the form

$$\frac{\partial u_s}{\partial s} + \frac{\partial(hu_n)}{\partial n} = 0, \tag{2.13}$$

$$\frac{\partial u_s}{\partial T} + \epsilon\Gamma u_n + \frac{\epsilon}{h}(u_s - c_s)\left[\frac{\partial u_s}{\partial s} + \epsilon MKu_n\right] + \epsilon(u_n - c_n)\frac{\partial u_s}{\partial n} + \frac{1}{h}\frac{\partial p}{\partial s} = \frac{1}{2}\delta^2\left[\frac{1}{h}\frac{\partial E_{ss}}{\partial s} + \epsilon\frac{2MK}{h}E_{ns} + \frac{\partial E_{ns}}{\partial n}\right], \tag{2.14}$$

$$\frac{\partial u_n}{\partial T} - \epsilon\Gamma u_s + \frac{\epsilon}{h}(u_s - c_s)\left[\frac{\partial u_n}{\partial s} - \epsilon MKu_s\right] + \epsilon(u_n - c_n)\frac{\partial u_n}{\partial n} + \frac{\partial p}{\partial n} = \frac{1}{2}\delta^2\left[\frac{1}{h}\frac{\partial E_{sn}}{\partial s} + \epsilon\frac{2MK}{h}E_{nn} + \frac{\partial E_{nn}}{\partial n}\right], \tag{2.15}$$

with boundary conditions

$$u_n = c_n, \quad E_{ns} = 0, \quad p = \zeta - F - \tfrac{1}{2}\delta^2 E_{nn}, \tag{2.16}$$

at $n = 0$. Here we have made the definitions

$$E_{ss} = \frac{2}{h}\left(\frac{\partial u_s}{\partial s} + \epsilon MKu_n\right), \quad E_{nn} = 2\frac{\partial u_n}{\partial n}, \tag{2.17a}$$

$$E_{ns} = E_{sn} = \frac{1}{h}\left(\frac{\partial u_n}{\partial s} - \epsilon MKu_s\right) + \frac{\partial u_s}{\partial n}, \tag{2.17b}$$

$$\Gamma = -\frac{1}{M^2}\frac{\partial^2\zeta}{\partial s\,\partial T}, \quad K = -\frac{1}{M^3}\frac{\partial^2\zeta}{\partial s^2}, \quad h = M(1+\epsilon Kn), \tag{2.18}$$

$$c_s = \Gamma n + \frac{\epsilon}{M}\frac{\partial\zeta}{\partial T}\frac{\partial\zeta}{\partial s}, \quad c_n = \frac{1}{M}\frac{\partial\zeta}{\partial T}, \tag{2.19}$$

where c_s ad c_n are dimensionless components of the speed $\boldsymbol{c}$ in (2.8), and Γ is the dimensionless version of the angular speed in (2.10).

3. Near-field outer solution

Since the flow in this region is irrotational, it can be computed if the normal components of velocity at the outer edges of the surface and bottom boundary layers are known. These layers are analysed in Appendix A, where it is shown that the flows

https://doi.org/10.1017/S002211209700520X Published online by Cambridge University Press

due to displacement thickness associated with the surface and bottom layers are $O(\delta^2/\epsilon)$ and $O(\delta)$, respectively. Therefore, because of the parameter restriction $\delta \ll \epsilon$, boundary layer pumping can be ignored if we are interested only in computing the $O(\epsilon)$ solution for the steady streaming velocity in the outer region.

To describe the motion we employ the coordinates (2.7). Then, using Joseph's method, we expand the pressure p and the Cartesian velocity components (u, w) in the form

$$f = f^{(0)} + \epsilon\left[f^{(1)} + \frac{z+d}{d}\zeta^{(0)}\frac{\partial f^{(0)}}{\partial z}\right\} + \ldots, \tag{3.1}$$

where $z = -d$ corresponds to $r_3 - d$, the bottom boundary, and $z = 0$ to $r_3 = \zeta$, the free surface. As explained in Joseph (1973) and Leibovitz (1982), the partial differential equations satisfied by the terms $f^{(m)}(x, z, t)$ are the same as if (x, z) are Cartesian coordinates.

The most convenient solution method is to express the velocity and pressure in terms of velocity potentials $\phi^{(m)}$ through

$$u^{(0)} = \frac{\partial\phi^{(0)}}{\partial x}, \quad w^{(0)} = \frac{\partial\phi^{(0)}}{\partial z}, \quad p^{(0)} = -\frac{\partial\phi^{(0)}}{\partial t}, \tag{3.2}$$

$$u^{(1)} = \frac{\partial\phi^{(1)}}{\partial x}, \quad w^{(1)} = \frac{\partial\phi^{(1)}}{\partial \mathrm{z}}, \quad p^{(1)} = -\frac{\partial\phi^{(1)}}{\partial t} - \tfrac{1}{2}\boldsymbol{u}^{(0)}\cdot\boldsymbol{u}^{(0)}, \tag{3.3}$$

where $\phi^{(0)}$ and $\phi^{(1)}$ solve Laplace's equation subject to

$$\frac{\partial\phi^{(0)}}{\partial z} = \frac{\partial\phi^{(1)}}{\partial z} = 0 \tag{3.4}$$

at $z = -d$, and

$$\frac{\partial\phi^{(0)}}{\partial z} = \frac{\partial\zeta^{(0)}}{\partial t}, \quad \frac{\partial\phi^{(1)}}{\partial z} = \frac{\partial\zeta^{(1)}}{\partial t} + \frac{\partial}{\partial x}\left(\frac{\partial\phi^{(0)}}{\partial x}\zeta^{(0)}\right), \tag{3.5}$$

$$p^{(0)} = \zeta^{(0)} - F, \quad p^{(1)} = \zeta^{(1)} + \zeta^{(0)}\frac{\partial^2\zeta^{(0)}}{\partial t^2}, \tag{3.6}$$

at $z = 0$. Here F takes the form

$$F = a(x)\exp(-\mathrm{i}\sigma t) + \text{c.c.}, \tag{3.7}$$

where a is even in x.

We ignore transients by taking the dependent variables to be periodic functions of σt. Then $\phi^{(0)}$ and $\zeta^{(0)}$ are given by

$$\phi^{(0)} = \phi^{[0]}(x, z)\exp(-\mathrm{i}\sigma t) + \text{c.c.}, \quad \zeta^{(0)} = \zeta^{[0]}(x)\exp(-\mathrm{i}\sigma t) + \text{c.c.}, \tag{3.8}$$

where $\phi^{[0]}$ solves Laplace's equation subject to the boundary conditions

$$\frac{\partial\phi^{[0]}}{\partial z} - \sigma^2\phi^{[0]} = -\mathrm{i}\sigma a \quad \text{at} \quad z = 0, \quad \frac{\partial\phi^{[0]}}{\partial z} = 0 \quad \text{at} \quad z = -d, \tag{3.9}$$

and to outgoing wave conditions at $|x| = \infty$. After $\phi^{[0]}$ has been computed, $\zeta^{[0]}$ can be determined using the first equation in (3.5).

In calculating the outer first-order mean flow, we let angle brackets denote the time average, and we define Φ by

$$\Phi = \langle\phi^{(1)}\rangle, \tag{3.10}$$

https://doi.org/10.1017/S002211209700520X Published online by Cambridge University Press

where Φ satisfies Laplace's equation subject to $\partial\Phi/\partial z = 0$ at $z = -d$ and

$$\frac{\partial \Phi}{\partial z} = \frac{\partial}{\partial x}\left\langle \frac{\partial \phi^{(0)}}{\partial x}\zeta^{(0)} \right\rangle \tag{3.11}$$

at $z = 0$. From these equations, it can be shown that the horizontal Stokes drift velocity

$$u^s = \left\langle \int u^{(0)}\,\mathrm{d}t\,\frac{\partial u^{(0)}}{\partial x} + \int w^{(0)}\,\mathrm{d}t\,\frac{\partial u^{(0)}}{\partial z} \right\rangle \tag{3.12}$$

and the mean current $\langle u^{(1)}\rangle$ satisfy

$$\int_{-d}^{0} u^s\,\mathrm{d}z = \langle u^{(0)}\zeta^{(0)}\rangle_{z=0}, \quad \int_{-d}^{0}\langle u^{(1)}\rangle\,\mathrm{d}z = -\langle u^{(0)}\zeta^{(0)}\rangle_{z=0}, \tag{3.13}$$

and therefore the vertical integral of the mass transport velocity

$$u^m = \langle u^{(1)}\rangle + u^s \tag{3.14}$$

vanishes, as required for overall conservation of mass.

To solve the above equations, we define the Fourier transform of the function a in (3.7) by

$$\hat{a} = \frac{1}{2\pi}\int_{-\infty}^{\infty} a(x)\,\mathrm{e}^{-\mathrm{i}kx}\,\mathrm{d}x, \tag{3.15}$$

and find that the $O(1)$ outer solution takes the form

$$\zeta^{[0]} = \int_{-\infty}^{\infty} \frac{k\tanh(kd)\,\hat{a}}{k\tanh(kd) - \sigma^2}\,\mathrm{e}^{\mathrm{i}kx}\,\mathrm{d}k, \tag{3.16}$$

$$\phi^{[0]} = \int_{-\infty}^{\infty} \frac{\mathrm{i}\sigma\hat{a}}{\sigma^2 - k\tanh(kd)}\frac{\cosh[k(z+d)]}{\cosh(kd)}\,\mathrm{e}^{\mathrm{i}kx}\,\mathrm{d}k. \tag{3.17}$$

For all $a(x)$ such that $\hat{a}$ is analytic on the real transform axis, the wave field and mean velocity satisfy

$$\zeta^{(0)} \to \chi\exp\{\mathrm{i}(\kappa x - \sigma t\} + \text{c.c.} + \text{evanescent terms}, \tag{3.18a}$$

$$\langle u^{(1)}\rangle \to -\frac{2\kappa}{\sigma d}|\chi|^2 + \text{evanescent terms}, \tag{3.18b}$$

$$\langle w^{(1)}\rangle \to 0 + \text{evanescent terms}, \tag{3.18c}$$

where the evanescent terms decay exponentially with $|x|$, where κ is the positive solution of

$$k\tanh(kd) = \sigma^2, \tag{3.19}$$

and where

$$\chi = 2\pi\mathrm{i}\frac{\kappa\hat{a}(\kappa)}{1 + 2\kappa d\,\mathrm{cosech}(\kappa d)}. \tag{3.20}$$

Here $\langle u^{(1)}\rangle$ is negative, since it must balance the mass flux in the positive x-direction associated with the Stokes drift. Equations (3.18a, b) serve as matching conditions for the far-field equations discussed in §4.

https://doi.org/10.1017/S002211209700520X Published online by Cambridge University Press

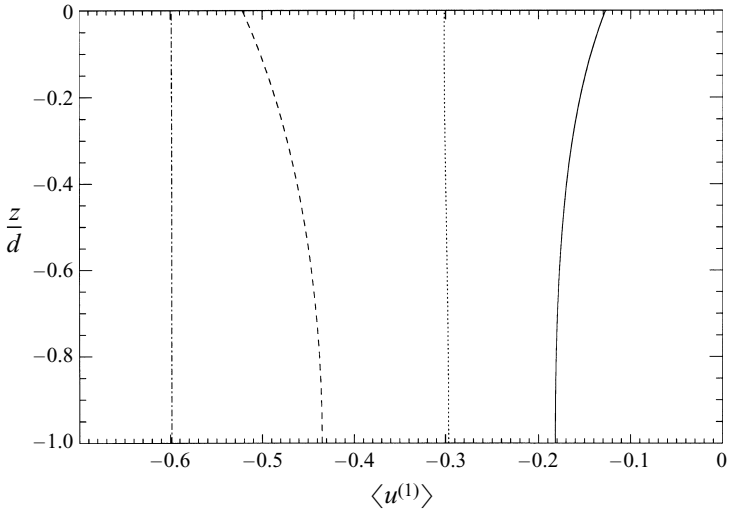


FIGURE 2. Vertical profiles of the near-field mean horizontal velocity. $\sigma = 1$, $d = 1$, $\lambda = 1$. ——, $x = 0.6563$; · · · · · ·, $x = 1.0405$ – – – –, $x = 1.5255$; -·-·-·, $x = 6.6286$.

Plots of the near-field mean horizontal velocity are given in figure 2 for the case $a = 2h\,\mathrm{sech}\,(x)$, $\sigma = 1$, and $d = 1$, with h chosen such that $|\chi| = \frac{1}{2}$. For this flow the solution for $u^{(1)}$ has essentially reached the asymptotic limit given by (3.18) at $x = 6.6286$.

4. Far-field outer solution

As stated previously, in treating the flow far from the wavemaker we invoke the parameter restriction (1.1), so that wave decay, nonlinear interactions, and thickening of the Stuart layers all take place on a horizontal length scale $O(1/\epsilon^2)$. With this in mind, we let κ denote the solution of (3.19) and we introduce the fast and slow variables

$$\theta = \kappa x - \sigma t, \quad X = \epsilon^2 x, \tag{4.1}$$

where (x, z) are defined in (2.7). In terms of these variables, the governing equations in the outer region are given with $O(\epsilon^6)$ errors by

$$\kappa\frac{\partial u}{\partial\theta} + \epsilon^2\frac{\partial u}{\partial X} + \frac{\partial w}{\partial z} = 0, \tag{4.2}$$

$$-\sigma\frac{\partial u}{\partial\theta} + \epsilon w\Omega + \kappa\frac{\partial P}{\partial\theta} + \epsilon^2\frac{\partial P}{\partial X} = \frac{1}{2}\lambda^2\epsilon^4\left(\kappa^2\frac{\partial^2 u}{\partial\theta^2} + \frac{\partial^2 u}{\partial z^2}\right), \tag{4.3}$$

$$-\sigma\frac{\partial w}{\partial\theta} - \epsilon u\Omega + \frac{\partial P}{\partial z} = \frac{1}{2}\lambda^2\epsilon^4\left(\kappa^2\frac{\partial^2 w}{\partial\theta^2} + \frac{\partial^2 w}{\partial z^2}\right), \tag{4.4}$$

where the total pressure P and the vorticity Ω are defined by

$$P = p + \tfrac{1}{2}\epsilon(u^2 + w^2), \quad \Omega = \frac{\partial u}{\partial z} - \kappa\frac{\partial w}{\partial\theta} - \epsilon^2\frac{\partial w}{\partial X}. \tag{4.5}$$

Expressing the lowest-order solution for the wave field as

$$\zeta^{(0)} = \zeta_{01}(X)\,E + \text{c.c.}, \tag{4.6}$$

https://doi.org/10.1017/S002211209700520X Published online by Cambridge University Press

where $E = \exp(\mathrm{i}\theta)$, and referring to the boundary layer analysis in Appendix A, we find that

$$\frac{\partial \langle u \rangle}{\partial z} = \epsilon \frac{8\kappa^3 |\zeta_{01}|^2}{\sigma} + O(\epsilon^2), \tag{4.7}$$

at $z = 0$, where angle brackets again denote time averaging. Also, since $\delta = O(\epsilon^2)$ and since viscous forces in the surface Stokes layer affect the outer flow at $O(\delta^2)$, as shown in Appendix A, the upper boundary conditions on the vertical velocity and pressure are the purely inviscid conditions

$$w = -\sigma \frac{\partial \zeta}{\partial \theta} + \epsilon\kappa \frac{\partial}{\partial \theta}(u\zeta) + \epsilon^2 \frac{\kappa}{2} \frac{\partial}{\partial \theta}\left(\zeta^2 \frac{\partial u}{\partial z}\right) + \epsilon^3 \left\{ \frac{\kappa}{6} \frac{\partial}{\partial \theta}\left(\zeta^3 \frac{\partial^2 u}{\partial z^2}\right) + \frac{\partial}{\partial X}(u\zeta) \right\} + O(\epsilon^4), \tag{4.8}$$

$$p = \zeta - \epsilon\zeta \frac{\partial p}{\partial z} - \epsilon^2 \frac{1}{2} \zeta^2 \frac{\partial^2 p}{\partial z^2} - \epsilon^3 \frac{1}{6} \zeta^3 \frac{\partial^3 p}{\partial z^3} + O(\epsilon^4), \tag{4.9}$$

at $z = 0$. The corresponding bottom boundary conditions are

$$\langle u \rangle = \epsilon \frac{6\kappa^2 |\zeta_{01}|^2}{\sigma \sinh(2\kappa d)} + O(\epsilon^2) \tag{4.10}$$

and

$$w = \epsilon^2 (Y_{01} E + \text{c.c.}) + O(\epsilon^3), \quad \langle w \rangle = O(\epsilon^4), \tag{4.11}$$

at $z = -d$, where

$$Y_{01} = \frac{\lambda\kappa^2(-1+\mathrm{i})}{2\sigma^{3/2}\cosh(\kappa d)} \zeta_{01}. \tag{4.12}$$

We now follow the procedure used by Davey & Stewartson (1974), and expand the dependent variables in the form

$$u = u_{01} E + \bar{u}_{01} \bar{E} + \epsilon(u_{10} + u_{11} E + \bar{u}_{11} \bar{E} + u_{12} E^2 + \bar{u}_{12} \bar{E}^2) + \ldots, \tag{4.13}$$

where an overbar denotes the complex conjugate. Our aim is to obtain equations governing the $O(1)$ surface elevation and the lowest-order non-vanishing approximation for the mean velocity components. In contrast to inviscid theories, which invariably yield indeterminate mean streaming velocities, our analysis involves no ambiguities.

The derivation of the surface elevation equation is lengthy, but presents no conceptual difficulties. The resulting evolution equation is

$$\frac{\partial \zeta_{01}}{\partial X} + \mathrm{i}\alpha |\zeta_{01}|^2 \zeta_{01} + [\beta + \mathrm{i}(\gamma - \beta)] \zeta_{01} = 0, \quad \zeta_{01} = \chi \quad \text{at} \quad X = 0, \tag{4.14}$$

where χ is the wave amplitude in (3.20) and where

$$\alpha = \frac{\kappa^4}{4C_g \sigma^3 \mu^2} [9 - 10\mu^2 + 9\mu^4 - 2\mu^2(1-\mu^2)^2], \tag{4.15}$$

$$\beta = \frac{\lambda\kappa\sigma^{1/2}}{2C_g \sinh(2\kappa d)}, \tag{4.16}$$

and

$$\gamma = \frac{2\kappa^2}{C_g \sinh(2\kappa d)} \int_{-d}^{0} u_{10}(X, z) \cosh[2\kappa(z+d)] \, \mathrm{d}z, \tag{4.17}$$

in which

$$\mu = \tanh(\kappa d), \quad C_g = \frac{\partial}{\partial \kappa} [\kappa \tanh(\kappa d)]^{1/2}. \tag{4.18}$$

https://doi.org/10.1017/S002211209700520X Published online by Cambridge University Press

Here the parameter α measures the nonlinearity of the waves, β is generated by the boundary layer pumping, and γ results from the Doppler effect produced by the mean horizontal velocity. In an inviscid theory, β would be zero and γ would be an *arbitrary* constant (see Mei 1989, section 12.3).

In the course of deriving (4.14), we found that $w_{10} = w_{20} = 0$. Proceeding to higher order, another lengthy calculation shows that the equations for the mean flow take the form

$$\frac{\partial u_{10}}{\partial X} + \frac{\partial w_{30}}{\partial z} = 0, \tag{4.19}$$

$$u_{10}\frac{\partial u_{10}}{\partial X} + (w_{30} + w^s)\frac{\partial u_{10}}{\partial z} + \frac{\partial \Pi}{\partial X} = \frac{1}{2}\lambda^2 \frac{\partial^2 u_{10}}{\partial z^2}, \tag{4.20}$$

$$\frac{\partial \Pi}{\partial z} = u^s \frac{\partial u_{10}}{\partial z}, \tag{4.21}$$

where
$$u^s = \frac{\partial S}{\partial z}, \quad w^s = -\frac{\partial S}{\partial X}, \quad S = \frac{2\kappa A^2 \sinh[2\kappa(z+d)]}{\sigma \sinh(2\kappa d)}, \tag{4.22}$$

$$\Pi = P_{30} - \tfrac{1}{2}u_{10}^2 + S\frac{\partial u_{10}}{\partial z}, \quad A = |\zeta_{01}|, \tag{4.23}$$

and where u_{10} and w_{30} are the lowest-order non-vanishing approximations for the mean velocity components. The boundary conditions on the mean flow are

$$\frac{\partial u_{10}}{\partial z} = \frac{8\kappa^3 A^2}{\sigma}, \quad w_{30} = \frac{2\kappa}{\sigma}\frac{\partial A^2}{\partial X} \quad \text{at} \quad z = 0, \tag{4.24}$$

$$u_{10} = \frac{6\kappa^2 A^2}{\sigma \sinh(2\kappa d)}, \quad w_{30} = 0 \quad \text{at} \quad z = -d, \tag{4.25}$$

$$u_{10} = -\frac{2\kappa}{\sigma d}|\chi|^2 \quad \text{at} \quad X = 0. \tag{4.26}$$

These equations differ slightly from the mean flow equations derived by Leibovich (1980) because in our far field the horizontal derivatives of the mean velocity are much smaller than vertical derivatives. Another difference is that in our theory the equations governing the wave amplitude and mean flow are coupled, since the solution of (4.14) depends on γ and hence on u_{10}, while the mean flow depends on A, the modulus of the wave amplitude ζ_{01}.

To compute ζ_{01}, we note that $\partial A^2/\partial X = -2\beta A^2$, so that

$$A = |\chi| \exp(-\beta X), \tag{4.27}$$

and from this result we find that

$$\zeta_{01} = \chi \exp[-R(X)], \quad R = \beta X + \mathrm{i}\left[\frac{\alpha}{2\beta}(|\chi|^2 - A^2) + \int_0^X \gamma(X')\,\mathrm{d}X'\right]. \tag{4.28}$$

Therefore, since γ is the only term in (4.28) depending on u_{10}, the mean flow affects only the phase of the wave amplitude, not its modulus.

The problem of computing the mean flow reduces now to solving (4.19)–(4.26), with A given by (4.27). When $|X|$ is large, the nonlinear terms and the terms involving u^s and

https://doi.org/10.1017/S002211209700520X Published online by Cambridge University Press

w^s in (4.19)–(4.21) are small due to viscous decay, and can be omitted. The mean horizontal velocity is then parabolic in z, and corresponds to the conduction solution of Longuet-Higgins, as corrected for viscous wave decay by Craik. Apart from this case, the mean flow must be computed numerically.

To simplify the numerical algorithm, we express the problem in terms of a stream function $\Psi(X, z)$ defined so that $u_{10} = \partial\Psi/\partial z$ and $w_{30} = -\partial\Psi/\partial X$. Letting subscripts denote partial differentiation, the governing equation for Ψ is

$$(\Psi_z + S_z)\,\Psi_{Xzz} - (\Psi_X + S_X)\,\Psi_{zzz} = \tfrac{1}{2}\lambda^2\,\Psi_{zzzz}, \tag{4.29}$$

with boundary conditions

$$\Psi(X, 0) = -S(X, 0), \quad \Psi_{zz}(X, 0) = \frac{8\kappa^3 A^2}{\sigma} \tag{4.30}$$

at the top surface,

$$\Psi(X, -d) = 0, \quad \Psi_z(X, -d) = \frac{6\kappa^2 A^2}{\sigma \sinh(2\kappa d)} \tag{4.31}$$

at the bottom, and

$$\Psi(0, z) = -S(0, 0)\frac{z + d}{d} \tag{4.32}$$

at $X = 0$.

The most straightforward method for solving (4.29)–(4.32) consists of marching forward in X using an implicit finite difference scheme for discretizing X-derivatives, and solving a nonlinear boundary value problem in z for each X. For small enough wave amplitudes we were able to solve the mean flow equations in this way and to verify that the mean horizontal velocity approaches a parabolic profile in z as $X \to \infty$. For larger amplitudes the iteration required to solve the boundary value problem in z refuses to converge, probably because the flow direction is opposite to the marching direction over a portion of the water column. Similar stability problems are discussed by Rubin & Tannehill (1992).

To compute the solution in the case of large-amplitude waves, we treated (4.29)–(4.32) through use of pseudospectral collocation in both X and z, with the grid point values of Ψ taken as the unknowns. Discretization of the z-derivatives was carried out by using a linear transformation to map the physical domain $z \in [-d, 0]$ into the computational domain $z_L \in [-1, 1]$ and by collocating on Chebyshev–Gauss–Lobotto points in z_L. Similarly, X-derivatives were treated by mapping $X \in [0, \infty)$ into $x_R \in [-1, 1]$ through use of the transformation

$$x_R = \frac{X - L}{X + L}, \tag{4.33}$$

where L is a positive constant, and by collocating on Chebyshev–Gauss–Radau points in x_R. As noted by Boyd (1989, p. 447), the boundary conditions at $X = \infty$ are 'natural' in the sense that they need not be explicitly imposed.

Differentiation matrices in the z_L-domain can be found in standard references (Canuto *et al.* 1988; Boyd 1989), and the matrix representing first derivatives with respect to x_R is given in our Appendix B. Differentiation matrices in the (X, z)-coordinates were computed using the chain rule, and were chosen to incorporate the boundary conditions.

The first step in the method used here for solving the spatially discretized equations consisted of multiplying all nonlinear terms by a parameter τ, so that $\tau = 0$ corresponds

https://doi.org/10.1017/S002211209700520X Published online by Cambridge University Press

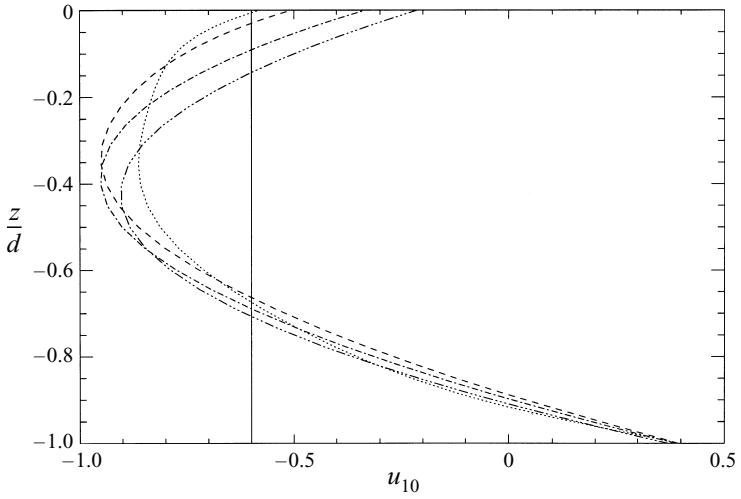


FIGURE 3. Vertical profiles of the far-field mean horizontal velocity. $\sigma = 1$, $d = 1$, $\lambda = 1$. ——, $X = 0$; · · · · · ·, $X = 0.003833$; – – – –, $X = 0.008905$; - · - · - ·, $X = 0.04292$; — · · · — · · · — · · ·, $X = 0.1713$.

to the linearized problem and $\tau = 1$ to the nonlinear problem. The resulting equations take the form

$$\boldsymbol{M}\boldsymbol{\Psi} + N(\boldsymbol{\Psi}, \tau) = \boldsymbol{c}, \tag{4.34}$$

where $\boldsymbol{\Psi}$ is a column vector whose entries are the values of $\boldsymbol{\Psi}$ at the grid points, $\boldsymbol{c}$ is a known column vector, $\boldsymbol{M}$ is a matrix with elements independent of $\boldsymbol{\Psi}$, and $N(\boldsymbol{\Psi}, \tau)$ is a nonlinear function of its arguments satisfying $N(\boldsymbol{\Psi}, 0) = 0$. Differentiating (4.34) with respect to τ yields an ordinary differential equation of $\boldsymbol{\Psi}$ with initial condition $\boldsymbol{\Psi}(0)$ obtained by solving (4.34) for $\tau = 0$. The solution $\boldsymbol{\Psi}(\tau)$ was then advanced in τ through use of a second-order Runge–Kutta scheme as a predictor step and solution of (4.34) by Newton iteration as a corrector step.

In the numerical simulations we used a 33×33 grid and varied the mapping parameter L in (4.33) depending on the wavelength. The accuracy of the scheme was controlled by imposing tolerances on the solution increment in the Newton iteration and on the residual of the nonlinear equation for each τ. These tolerances were set at 10^{-8} and 10^{-6}, respectively. In contrast to our experience in using the marching method, no difficulties were encountered in computing $\boldsymbol{\Psi}(1)$, the solution of the original system of nonlinear equations.

As typical examples of mean horizontal velocity profiles, we give in figure 3 the solution for the case $A(X = 0) = 0.5$, $\sigma = 1$, $d = 1$, and $\lambda = 1$ for different values of X. As can be seen, the solution changes from a depth-independent profile to a parabolic profile as X increases. In figure 4 we show the difference between our results for this case and Craik's theory, the solution to $\partial^4 \boldsymbol{\Psi}/\partial z^4 = 0$ with boundary conditions (4.30) and (4.31). As anticipated, the linear and nonlinear solutions are indistinguishable far enough downstream. Because the only difference between Craik's solution and Longuet-Higgins' theory consists of the inclusion of viscous wave decay in Craik's work, the shape of our velocity profile far from the wavemaker solution also agrees with the conduction solution of Longuet-Higgins.

Since the evolution to the conduction solution is relatively rapid in this case, our theory validates Craik's approximation. However, for larger depths or smaller wavelengths, the evolution to the conduction solution is less rapid. For example, for one of the experiments of Mei, Liu & Carter (1972) discussed below, $\sigma = 1$, $d = 2.01$,

https://doi.org/10.1017/S002211209700520X Published online by Cambridge University Press

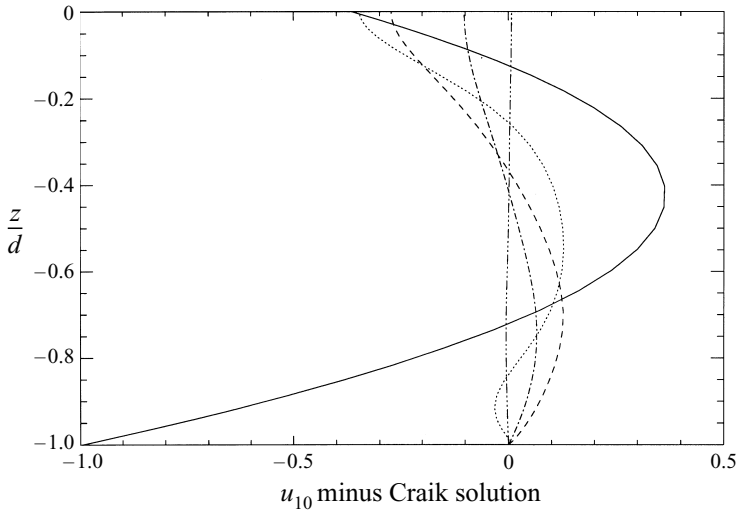


FIGURE 4. Vertical profiles of the far-field mean horizontal velocity minus Craik's (1982) solution. $\sigma = 1, d = 1, \lambda = 1$. ——, $X = 0$; · · · · · · · , $X = 0.003833$; – – – –, $X = 0.008905$; -·-·-·-, $X = 0.04292$; —· · ·—· · ·—· · ·, $X = 0.1713$.

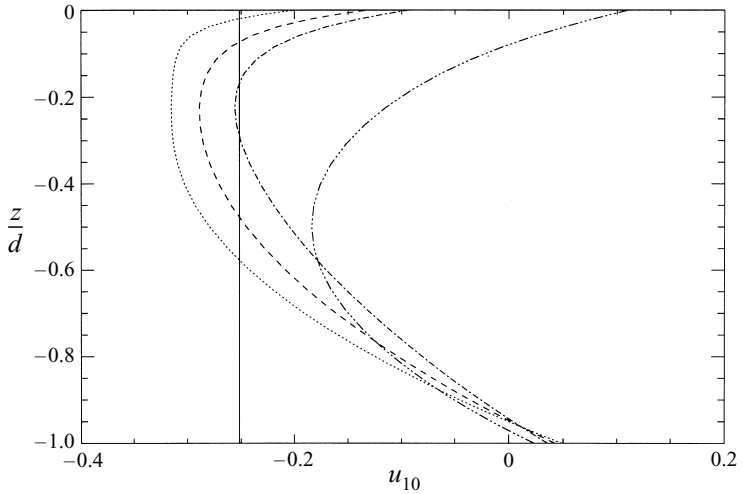


FIGURE 5. Vertical profiles of the far-field mean horizontal velocity. $\sigma = 1.00$, $\kappa = 1$, $d = 2.01$, $\lambda = 0.242$, $\epsilon = 0.155$. ——, $X = 0$; · · · · · · · , $X = 7.578$; – – – –, $X = 16.38$; -·-·-·-, $X = 27.42$; —· · ·—· · ·—· · ·, $X = 54.26$.

$\kappa = 1$, and $\lambda = 0.242$. In figures 5 and 6 we show the corresponding plots for this case. Because the dimensionless depth is larger and λ is smaller than for the flow discussed in the previous paragraph, the right-hand side of (4.29) is smaller in the present case. Therefore, in this example $\partial^4 \Psi / \partial z^4 = 0$ is a poor approximation to equation (4.29) except very far from the wavemaker, and Craik's solution only holds in this region.

5. Comparison of far-field flow with observations

Probably the most extensive set of laboratory observations of mass transport in water waves are those carried out by Mei, Liu, and Carter (1972, hereafter referred to as MLC). Most of their measurements were taken several wavelengths from the

https://doi.org/10.1017/S002211209700520X Published online by Cambridge University Press

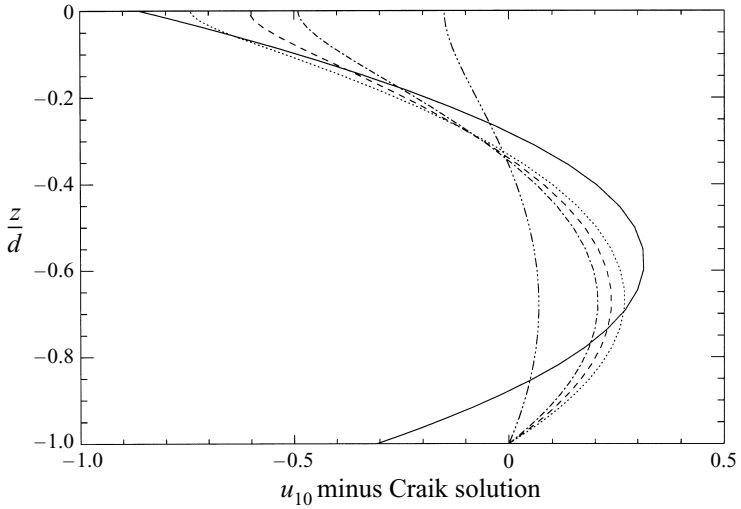


FIGURE 6. Vertical profiles of the far-field mean horizontal velocity minus Craik's (1982) solution. $\sigma = 1.00$, $\kappa = 1$, $d = 2.01$, $\lambda = 0.242$, $\epsilon = 0.155$. ——, $X = 0$; · · · · · ·, $X = 7.578$; – – – –, $X = 16.38$; -·-·-·, $X = 27.42$; —· · ·—· · ·—· · ·, $X = 54.26$.

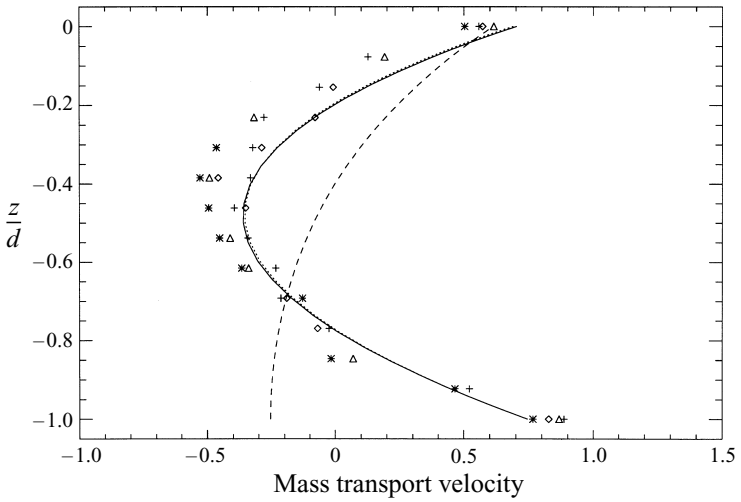


FIGURE 7. Mass transport velocity profiles. $k = 1$, $d = 1.02$, $\sigma = 0.886$, $\lambda = 0.496$, $\epsilon = 0.0863$. Station 2, $X = 0.205$. ——, Present theory; · · · · · ·, Craik solution; – – – –, Stokes solution; experimental data points from MLC: +, time = 1 h; *, time = 1 h; ◇, time = 2 h; △, time = 2 h.

wavemaker. Our theory predicts that at these distances the characteristics of the wavemaker do not affect the flow, so that MLC's use of a paddle wavemaker presents no problems in comparing our theory with their observations.

In his paper, Craik lists a number of problems in making such comparisons, in particular effects due to large wave amplitudes and to evolution of the mean velocity profile with distance from the wavemaker. Our theory alleviates the first problem by including finite-amplitude effects, and the second by including the variation of the mean profile with horizontal distance. However, we have not considered other factors discussed by Craik, namely effects due to surface contamination, channel sidewalls, temporal evolution, and the influence of air flow on the motion.

MLC measured mass transport velocities at various positions in the water column.

https://doi.org/10.1017/S002211209700520X Published online by Cambridge University Press

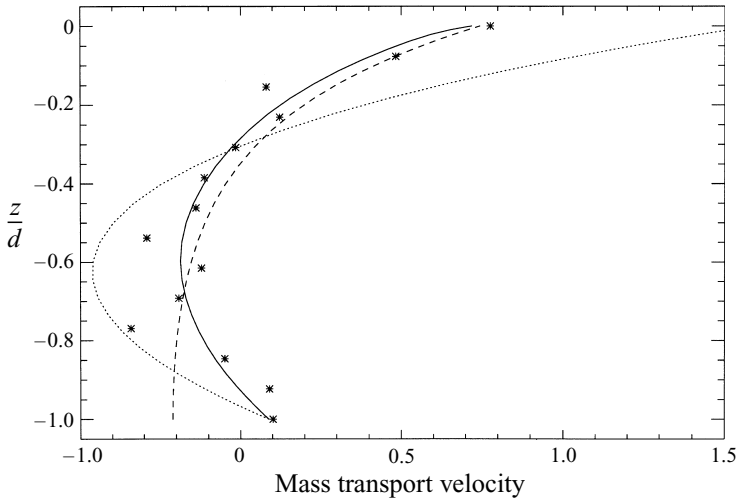


FIGURE 8. Mass transport velocity profiles. $k = 1$, $d = 2.01$, $\sigma = 1.00$, $\lambda = 0.242$, $\epsilon = 0.155$. Station 2, $X = 1.29$. ——, present theory; · · · · · ·, Craik solution; – – – –, Stokes solution; experimental data points from MLC: *, time = 18 h.

Most of their data were taken from Station 2, located 3.5 m downstream from the wavemaker. However, for some of the shorter waves they also provide data at other stations. In our calculation, we need the amplitude of the wave at $X = 0$. For each of our simulations, the scaling wavenumber and amplitude were taken from the station closest to the wavemaker, and equation (4.27) was used to obtain the amplitude at $X = 0$. This difference in amplitude was very small for most cases, consistent with the remarks in MLC.

Figures 7 and 8 show a comparison of the MLC measurements of the mass transport velocity with the present computation, the irrotational theory of Stokes, and the linear theory of Craik. Figure 7 depicts a case at a station for which the flow is effectively linear, and for which the differences between our solution and Craik's are negligible. In figure 8, we show a flow which has a larger effective depth; neither at this station nor at the others does the profile resemble the conduction solution, and this is typical of these cases. Thus, the advantage of our theory is clear: it contains the conduction solution as a special case but it also retains nonlinear terms which are significant except very far from the wavemaker.

6. Discussion

Our results suggest that the flow near the wavemaker consists of an irrotational core bounded by double boundary layer structures at the top and bottom boundaries. Each structure is made up of Stokes layers in which the time-dependent part of the vorticity decays to zero with distance from the boundary on an $O(\delta)$ dimensionless length scale, and Stuart layers in which the steady part of the vorticity decays on an $O(\delta/\epsilon)$ dimensionless scale. In this near-field region the mean flow outside the boundary layers closely resembles Stokes' irrotational solution.

The Stuart layers thicken with distance from the wavemaker, much like the Blasius boundary layers near the entrance to a channel, and eventually fill the fluid column. In this far-field region, the mean flow is essentially the same as predicted by Longuet-Higgins' viscous conduction solution. Thus, our resolution of the disagreement between the theories of Stokes and Longuet-Higgins is that both solutions are correct,

https://doi.org/10.1017/S002211209700520X Published online by Cambridge University Press

but in different parts of the flow domain. The Stokes solution for the mean flow is valid near the wavemaker because vorticity in this region is confined to the boundary layers, and the Longuet-Higgins conduction solution holds in the far field because the horizontal length scale for the mean flow in this region is large and the effective Reynolds number for the mean flow is small.

The mean horizontal flow in the region between the inviscid near field and viscous far field varies slowly with the horizontal coordinate, but eventually evolves to Longuet-Higgins' conduction solution far downstream. Flows with small depth to wavelength ratios reach the conduction solution in shorter distances than deep water flows because of the enhanced importance of viscous forces in the shallow water case.

For a more realistic model of the flow in wave tanks than given here, it would be necessary to include the effect of sidewalls, of a flap or wedge type wavemaker, of surfactants, and of the air flow. We have instead concentrated on resolving the differences between the theories of Stokes and Longuet-Higgins, with all extraneous effects omitted.

In virtually all experiments known to the authors, the mean and mass transport velocities are measured far from the wavemaker, and the conduction solution is invariably observed. With regard to verification of the present theory, it would be useful to repeat these experiments to see if Stokes-type profiles occur in the near field and if these solutions evolve into the Longuet-Higgins conduction solution profiles, as predicted above.

This work was sponsored under the Program in Ocean Surface Processes and Remote Sensing at the University of Michigan, funded under the University Research Initiative of the Office of Naval Research, Contract No. N00014-92-JI650.

Appendix A. Surface and bottom boundary layers

In treating the flow in the boundary layers we will provide only the asymptotic structure and the key equations.

To analyse the surface layer, we employ a boundary layer theory of additive type by letting (U, W, Q) denote the outer solution for (u_s, u_n, p) and by expressing the dependent variables in the form

$$u_s = u + U, \quad u_n = w + W, \quad p = q + Q. \tag{A 1}$$

Here u, w, and q depend on $z = n/\delta$ and vanish as z tends to $-\infty$, and U, W, and Q depend on the unstretched coordinate n. The governing equations are (2.11)–(2.19).

We now let $x = s$, substitute A 1) into these equations, and expand the solution in the form

$$u = u(z) = u_0(z) + \delta u_1(z) + \ldots, \quad U = U(n) = U_0(n) + \delta U_1(n) \ldots, \tag{A 2}$$

where (u, w, q) and (U, W, Q) depend on x and T in addition to z or n. Carrying out this procedure and noting that the outer dependent variables solve (2.13)–(2.15), we find that

$$u_0 = 0, \quad w_0 = w_1 = 0, \quad q_0 = q_1 = 0, \tag{A 3}$$

so that the boundary conditions become

$$W_0 = c_{n0}, \quad W_1 = c_{n1}, \quad W_2 + w_2 = c_{n2}, \tag{A 4a–c}$$

$$Q_0 = \zeta_0 - F, \quad Q_1 = \zeta_1, \quad Q_2 + q_2 = \zeta_2 - \frac{\partial W_0}{\partial n}, \tag{A 4d–f}$$

$$\frac{\partial u_1}{\partial z} + \frac{\partial U_0}{\partial n} + \frac{1}{M_0}\frac{\partial c_{n0}}{\partial z} - \epsilon K_0 U_0 = 0, \tag{A 5}$$

https://doi.org/10.1017/S002211209700520X Published online by Cambridge University Press

at $n = z = 0$. Equation (A 5) can also be expressed in the form

$$\frac{\partial u_1}{\partial z} + \Omega_0 + 2\left\{\frac{1}{M_0}\frac{\partial c_{n0}}{\partial \mathrm{x}} - \epsilon K_0 U_0\right\} = 0, \tag{A 6}$$

where Ω_0 is the $O(1)$ term in the expansion of the r_2-component of the outer vorticity in powers of δ, and where U_0, W_0, and their derivatives in (A 6) and in subsequent equations are evaluated at $n = 0$.

It is easily shown that the $O(\delta)$ continuity and normal momentum equations take the form

$$\frac{\partial w_2}{\partial z} = -\frac{1}{M_0}\frac{\partial u_1}{\partial x}, \quad \frac{\partial q_2}{\partial z} = 2\epsilon\{\Gamma_0 + \epsilon K_0(U_0 - c_{s0})\}\, u_1, \tag{A 7}$$

with boundary conditions $w_2 = q_2 = 0$ at $z = -\infty$, and therefore w_2 and q_2 can be determined by integration over z. Substituting the values of these variables at $z = 0$ into (A 4c, f) then provides boundary conditions on W_2 and Q_2 at $n = 0$ if u_1, ζ_0, U_0, and W_0 are known.

A longer but still straightforward calculation yields an equation for u_1:

$$\frac{\partial u_1}{\partial T} + \frac{\epsilon}{M_0}\left\{(U_0 - c_{s0})\frac{\partial u_1}{\partial x} + \left(\frac{\partial U_0}{\partial x} + \epsilon M_0 K_0 c_{n0}\right)u_1\right\} + \epsilon z \frac{\partial W_0}{\partial n}\frac{\partial u_1}{\partial z} = \frac{1}{2}\frac{\partial^2 u_1}{\partial z^2}. \tag{A 8}$$

Use of the outer continuity equation evaluated at $n = 0$ shows that (A 8) can also be expressed as

$$\frac{\partial u_1}{\partial T} - \frac{1}{2}\frac{\partial^2 u_1}{\partial z^2} = -\frac{\epsilon}{M_0}\left\{(U_0 - c_{s0})\frac{\partial u_1}{\partial x} + \left(\frac{\partial U_0}{\partial x} + \epsilon M_0 K_0 c_{n0}\right)\left(u_1 - z\frac{\partial u_1}{\partial z}\right)\right\}, \tag{A 9}$$

and solution of this equation subject to (A 6) and $u_1 = 0$ at $z = -\infty$ determines the $O(\delta)$ tangential component of velocity in the surface boundary layer.

It can be verified that the present theory is applicable for the parameter range $\delta \ll O(1)$, $\epsilon \leqslant O(1)$, and that the above equations remain valid as they stand if viscous decay of the waves is taken into account by letting the solution depend on the slow variable $X = \delta x$. Hence (A 7) and (A 9) are valid for small- or finite-amplitude waves decaying under the influence of bottom friction.

If the wave amplitude is small, as in the present problem, further results can be obtained by expanding u_1 in the form

$$u_1 = u_1^{(0)} + \epsilon u_1^{(1)} + \ldots. \tag{A 10}$$

In what follows we assume that ζ_0 and U_0 are given to lowest order by

$$\zeta_0^{(0)} = a(x)\, \mathrm{e}^{-\mathrm{i}\sigma T} + \text{c.c.}, \quad U_0^{(0)} = b(x)\, \mathrm{e}^{-\mathrm{i}\sigma T} + \text{c.c.}, \tag{A 11}$$

where c.c. denotes the complex conjugate, and that the vorticity Ω_0 vanishes to lowest order in an expansion in powers of ϵ.

Solution of the equations obtained by substituting (A 10) into (A 9) is straightforward, and ultimately yields the results

$$u_1^{(0)} \to c(x), \quad u_1^{(1)} \to \alpha z + d(x), \tag{A 12}$$

as $z \to -\infty$, in which

$$\alpha = 4\left\langle \frac{\partial U_0^{(0)}}{\partial x}\frac{\partial \zeta_0^{(0)}}{\partial x}\right\rangle - \langle \Omega_0^{(1)} \rangle, \tag{A 13}$$

https://doi.org/10.1017/S002211209700520X Published online by Cambridge University Press

where the angle brackets denote the time average and where $c(x)$ and $d(x)$ remain to be determined. It would seem that the requirement $u \to 0$ as $z \to -\infty$ implies that $c = d = \alpha = 0$, as suggested by Longuet-Higgins. However, in deriving (A 12) we have retained terms $O(\epsilon\delta)$ in the tangential momentum equation and omitted terms $O(\delta^2)$, and therefore (A 12) is valid only if $\delta \ll \epsilon$. In this case the outer equations for the mean flow are inviscid, and are incompatible with the boundary condition on the vorticity implied by setting $\alpha = 0$. Consequently, the expansion (A 10) cannot be uniformly valid, and instead we assume that a Stuart layer lies between the Stokes layer and the outer region.

To derive the equations for the Stuart layer, we let $Z = \epsilon z$ denote a stretched normal coordinate, and again expand u_1 in powers of ϵ. From (A 9) we find that u_1 is given by

$$u_1 = A(x, Z) + \epsilon\left\{B(x, Z) - \int^T f(x, Z, T')\,\mathrm{d}T'\right\} + O(\epsilon^2), \tag{A 14}$$

where the integral has vanishing time average and where

$$f = U_0^{(0)}\frac{\partial A}{\partial x} + \frac{\partial U_0^{(0)}}{\partial x}\left(A - Z\frac{\partial A}{\partial Z}\right). \tag{A 15}$$

Matching the outer and inner solutions thus gives

$$\left.\frac{\partial A}{\partial Z}\right|_{Z=0} = \alpha, \quad c(x) = A\,|_{Z=0}, \tag{A 16}$$

in which the first relation provides a boundary condition for A and the second gives the function $c(x)$ in (A 12) after A has been determined.

The governing equation for A is obtained by averaging the $O(\epsilon^2)$ Stuart layer version of (A 9) over time. This lengthy calculation yields

$$U^m\frac{\partial A}{\partial x} + \frac{\partial U^m}{\partial x}\left(A - Z\frac{\partial A}{\partial Z}\right) = \frac{1}{2}\frac{\partial^2 A}{\partial Z^2}, \tag{A 17}$$

where U^m is the outer horizontal mass transport velocity evaluated at the unperturbed water surface, and where A satisfies (A 16) and the condition $A \to 0$ as $Z \to -\infty$. It can be seen that (A 17) admits the solution $A \equiv 0$ if the $O(\epsilon)$ outer vorticity and the time average on the right-hand side of (A 13) vanish, as in the case of unforced irrotational standing waves (Dore 1976). In general, however, a non-trivial Stuart layer flow at the fluid surface is required. If so, (A 7) and (A 14) imply that the expansions of w_2 and q_2 begin with terms $O(\epsilon^{-1})$, and hence the flow due to displacement thickness and the pressure correction due to the presence of the boundary layer are both $O(\delta^2/\epsilon)$.

To treat the flow in the bottom layer we let $x = r_1$ and $z = (r_3 + d)/\delta$, where r_1 and r_3 are the horizontal and vertical Cartesian coordinates, and we express the corresponding velocity components as u and δw. Then, letting U denote the $O(\delta^0)$ outer horizontal velocity evaluated at $r_3 = -d$ and omitting terms $O(\delta^2)$, u and w solve the Prandtl equations

$$\frac{\partial u}{\partial x} + \frac{\partial w}{\partial z} = 0, \tag{A 18}$$

$$\frac{\partial u}{\partial t} + \epsilon\left(u\frac{\partial u}{\partial x} + w\frac{\partial u}{\partial z}\right) = \frac{1}{2}\frac{\partial^2 u}{\partial z^2} + \frac{\partial U}{\partial t} + \epsilon U\frac{\partial U}{\partial x}, \tag{A 19}$$

https://doi.org/10.1017/S002211209700520X Published online by Cambridge University Press

with boundary conditions $u = w = 0$ at $z = 0$, and $u \to U$ as $z \to \infty$.

If ϵ is small and if U has the form (A 11), with T replaced by t, use of a perturbation expansion in powers of ϵ shows that

$$\langle u \rangle \to \frac{3\epsilon}{2\sigma}\left\{2\mathrm{Im}\left(\bar{b}\frac{\partial b}{\partial x}\right) - \frac{\partial |b|^2}{\partial x}\right\} + O(\epsilon^2), \quad \langle w \rangle \to O(\epsilon), \tag{A 20}$$

as $z \to \infty$. As in our treatment of the surface layer, our view is that the first relation in (A 20) and the boundary condition $u \to U$ as $z \to \infty$ do not prescribe the value of $\langle U \rangle$ at the bottom of the core region, but instead imply non-uniform validity of the expansion in powers of ϵ. As before, this result indicates that a Stuart layer lies just outside the Stokes layer.

In treating the Stuart layer equations we take $Z = \epsilon z$ as the vertical coordinate. Then, expanding u, w, and U in series of the form

$$u = u^{(0)} + \epsilon u^{(1)} + \ldots, \quad w = \epsilon^{-1} w^{(-1)} + w^{(0)} + \epsilon w^{(1)} + \ldots, \tag{A 21}$$

where U has the same form of expansion as u, we find that

$$u^{(0)} = U^{(0)}, \quad w^{(-1)} = -Z\frac{\partial U^{(0)}}{\partial x}, \tag{A 22}$$

and

$$u^{(1)} = U^{(1)} + A(x, Z), \quad u^{(2)} = U^{(2)} + B(x, Z) + \hat{u}(x, Z, t). \tag{A 23}$$

Here

$$\hat{u} = -\xi\frac{\partial A}{\partial x} - \frac{\partial \xi}{\partial x}\left(A - Z\frac{\partial A}{\partial Z}\right), \tag{A 24}$$

where ξ solves $\partial \xi/\partial t = U^{(0)}$ subject to $\langle \xi \rangle = 0$, and can be regarded as the lowest-order approximation to the horizontal particle displacement at the outer edge of the bottom Stuart layer.

Averaging the continuity equation yields

$$\frac{\partial}{\partial x}\{A + \langle U^{(1)} \rangle\} + \frac{\partial}{\partial Z}\langle w^{(0)} \rangle = 0, \tag{A 25}$$

and the equation governing A is obtained by averaging the $O(\epsilon^3)$ horizontal momentum equation. The equations for $w^{(0)}$ and A can be case in a convenient form by defining the quantities

$$U^m = \left\langle U^{(1)} + \xi\frac{\partial U^{(0)}}{\partial x}\right\rangle, \quad u^m = U^m + A, \quad w^m = \left\langle w^{(0)} - Z\xi\frac{\partial^2 U^{(0)}}{\partial x^2}\right\rangle, \tag{A 26}$$

where U^m is the horizontal mass transport velocity just outside the Stuart layer and u^m and w^m are the lowest-order approximations to the horizontal and vertical mass transport velocities within the layer. When expressed in terms of these variables, the equations describing the flow in the Stuart layer become

$$\frac{\partial u^m}{\partial x} + \frac{\partial w^m}{\partial Z} = 0, \tag{A 27}$$

$$u^m\frac{\partial u^m}{\partial x} + w^m\frac{\partial u^m}{\partial Z} = \frac{1}{2}\frac{\partial^2 u^m}{\partial Z^2} + U^m\frac{\partial U^m}{\partial x}, \tag{A 28}$$

https://doi.org/10.1017/S002211209700520X Published online by Cambridge University Press

with boundary conditions $u^m \to U^m$ as $Z \to \infty$ and

$$\langle u^m \rangle \to \frac{1}{2\sigma}\left\{10\ \mathrm{Im}\left(\bar{b}\frac{\partial b}{\partial x}\right) - 3\frac{\partial |b|^2}{\partial x}\right\}, \quad \langle w^m \rangle \to 0, \tag{A 29}$$

as $Z \to 0$.

The flow due to displacement thickness out of the bottom Stuart layer is $O(\delta)$, as compared to the $O(\delta^2/\epsilon)$ flow due to the displacement thickness out of the surface Stuart layer. Hence, since the present theory is based on the parameter restriction $\delta \ll \epsilon$, the flows due to displacement thickness out of both Stuart layers can be ignored for the purpose of computing the outer near-field flow up to and including $O(\epsilon)$ terms. In the far field, the Stuart layers fill the fluid, and the appropriate boundary conditions at the outer edges of the Stokes layers are obtained by setting $\alpha = 0$ in (A 13) to obtain (4.7) in the text, and by applying (A 20) to obtain (4.10).

Appendix B. Differentiation matrix at the Radau points

The Chebyshev–Gauss–Radau points are

$$x_k = -\cos\left[\frac{2\pi(k-1)}{2N-1}\right], \quad k = 1, \ldots, N, \tag{B 1}$$

and the differentiation matrix D_{ik} is defined by

$$\left.\frac{\partial f}{\partial x}\right|_{x=x_i} = \sum_{k=1}^{N} D_{ik} f(x_k). \tag{B 2}$$

This is given by

$$D_{ik} = \frac{c_i}{c_k}(-1)^{k-i}\frac{(1-x_k)^{1/2}}{(1-x_i)^{1/2}}\frac{1}{x_i - x_k}, \quad i \neq k, \tag{B 3a}$$

$$D_{ik} = \frac{1}{2(1-x_k^2)}, \qquad i = k \neq 1, \tag{B 3b}$$

$$D_{ik} = -\tfrac{1}{3}N(N-1), \qquad i = k = 1, \tag{B 3c}$$

where, letting δ_{ik} denote the Kronecker delta,

$$c_k = 1 + \delta_{1k}. \tag{B 4}$$

REFERENCES

Boyd, J. P. 1989 *Chebyshev and Fourier Spectral Methods*. Springer.

Canuto, C., Hussaini, M. Y., Quarteroni, A. & Zang, T. A. 1988 *Spectral Methods in Fluid Dynamics*. Springer.

Craik, A. D. D. 1982 The drift velocity of water waves. *J. Fluid Mech.* **116**, 187–205.

Davey, A. & Stewartson, K. 1974 On three-dimensional packets of surface waves. *Proc. R. Soc. Lond.* A **338**, 101–110.

Dore, B. D. 1976 Double boundary layers in standing surface waves. *Pageoph.* **114**, 629–637.

Dore, B. D. 1977 On mass transport velocity due to progressive waves. *Q. J. Mech. Appl. Maths* **30**, 157–173.

Grimshaw, R. 1981 Mean flows generated by a progressing water wave packet. *J. Austral. Math. Soc.* B **22**, 318–347.

Iskandarani, M. & Liu, P. L.-F. 1991*a* Mass transport in two-dimensional water waves. *J. Fluid Mech.* **231**, 395–415.

https://doi.org/10.1017/S002211209700520X Published online by Cambridge University Press

Iskandarani, M. & Liu, P. L.-F. 1991*b* Mass transport in three-dimensional water waves. *J. Fluid Mech.* **231**, 417–437.

Iskandarani, M. & Liu, P. L.-F. 1993 Mass transport in a wave tank. *J. Waterway, Port, Coastal, Ocean Engng ASCE* **119**, 88–104.

Joseph, D. D. 1973 Domain perturbations: the higher order theory of infinitesimal water waves. *Arch. Rat. Mech. Anal.* **51**, 295–303.

Keller, H. B. 1970 A new difference scheme for parabolic problems. In *Numerical Solutions of Partial Differential Equations*, Vol. 2 (ed. B. Hubbard), pp. 327–350. Academic.

Leibovich, S. 1980 On wave–current interaction theories of Langmuir circulations. *J. Fluid Mech.* **99**, 715–724.

Leibovitz, N. R. 1982 Perturbation expansions on perturbed domains. *SIAM Rev.* **24**, 381–400.

Lighthill, M. J. 1978 *Waves in Fluids*. Cambridge University Press.

Liu, A.-K. & Davis, S. H. 1977 Viscous attenuation of mean drift in water waves. *J. Fluid Mech.* **81**, 63–84.

Longuet-Higgins, M. S. 1953 Mass transport in water waves. *Phil. Trans. R. Soc. Lond.* A **245**, 535–581.

Mei, C. C. 1989 *The Applied Dynamics of Ocean Surface Waves*. World Scientific.

Mei, C. C., Liu, P. L-F. & Carter, T. G. 1972 Mass transport in water waves. *Rep.* 146. Ralph M. Parsons Lab. Water Resources Hydrodynamics, MIT (referred to herein as MLC).

Rayleigh, Lord 1945 *The Theory of Sound*, 2nd edn. Dover.

Rubin, S. G. & Tannehill, J. C. 1992 Parabolized/reduced Navier–Stokes computational techniques. *Ann. Rev. Fluid Mech.* **24**, 117–144.

Stokes, G. G. 1847 On the theory of oscillatory waves. *Trans. Camb. Phil. Soc.* **8**, 441–455.

Stuart, J. T. 1966 Double boundary layers in oscillatory viscous flow. *J. Fluid Mech.* **24**, 673–687.

Van Dyke, M. D. 1970 Entry flow in a channel. *J. Fluid Mech.* **44**, 813–823.

Wen, J. & Liu, P. L.-F. 1994 Mass transport under partially reflected waves in a rectangular channel. *J. Fluid Mech.* **266**, 121–145.

https://doi.org/10.1017/S002211209700520X Published online by Cambridge University Press